J. Phys. D: Appl. Phys. **41** (2008) 135105 (6pp) doi:10.1088/0022-3727/41/13/135105

Mid-IR transmission of a large-area 2D silicon photonic crystal slab

L Prodan[1,2,8], R Hagen[1], P Gross[1,3], R Arts[1], R Beigang[4], C Fallnich[3,5], A Schirmacher[5], L Kuipers[6,7] and K-J Boller[1]

[1] Laser Physics and Nonlinear Optics Group, Department of Science and Technology, and MESA+ Research Institute, University of Twente, PO Box 217, 7500 AE Enschede, The Netherlands
[2] Laser Applicatie Centrum, University of Twente, Drienerlolaan 5, 7522 NB Enschede, The Netherlands
[3] Westfälische Wilhelms-Universität, Institute of Applied Physics, Corrensstr. 2-4, 48149 Münster, Germany
[4] Universität Kaiserslautern, Fachbereich Physik, Erwin-Schrödinger-Str., 67653 Kaiserslautern, Germany
[5] PTB Braunschweig, Spektrometrie und mikrooptische Messtechnik, Bundesallee 100, 38116 Braunschweig, Germany
[6] Optical Sciences Group, Department of Science and Technology, and MESA+ Research Institute, University of Twente, PO Box 217, 7500 AE Enschede, The Netherlands
[7] Center for Nanophotonics, FOM-Institute for Atomic and Molecular Physics AMOLF, Kruislaan 407, 1098 SJ Amsterdam, The Netherlands

E-mail: L.Prodan@tnw.utwente.nl

Received 25 February 2008, in final form 18 April 2008
Published 12 June 2008
Online at stacks.iop.org/JPhysD/41/135105

Abstract
We investigate the spectral transmission of a large-area ($10 \times 10\,\mathrm{mm}^2$) two-dimensional silicon-based photonic crystal (PhC) slab waveguide, which was fabricated by a laser interference lithography (LIL) using a silicon-on-insulator wafer. The slab carries a 1 μm period square pattern of round holes in the 0.5 μm thick silicon top layer. Transmission was recorded over the wavelength range from 1.1 to 2.4 μm, i.e. from the near-infrared single-photon absorption edge of silicon to below the mid-infrared two-photon absorption edge. Under normal incidence, we observe Fano and Fabry–Perot-type transmission resonances, in agreement with predictions based on coupled wave analysis. To determine the quality of the LIL fabrication process, the bandwidth of the transmission peaks is determined from experimental data and compared with results of the finite-difference time-domain analysis.

(Some figures in this article are in colour only in the electronic version)

1. Introduction

Photonic crystals are artificial materials with a strong variation of the refractive index in up to three space dimensions [1], enabling manipulation of light propagation, such as for realizing sensing devices [2], micro-lasers [3] or micro-cavities [4]. Of particular interest for spectral filtering applications are photonic crystal slabs (two-dimensional PhCs), where guided resonances should provide Fano-type transmission line shapes of narrow bandwidth superimposed on a broader and smoothly varying Fabry–Perot-type background [5]. Transmission measurements with free-standing (air-bridged) chalcogenide glass membranes confirmed these predictions [6]. Further investigations with free-standing silicon nitride membranes showed that the frequency of certain transmission resonances does not vary with the angle of incidence [7], which is of considerable interest for filtering of light comprising a wider angular spread.

However, the described 2D-PhCs [6, 7] only consist of a microscopically small area of about $100 \times 100\,\mu\mathrm{m}^2$. The resulting disadvantage is that the light to be filtered has to be of high spatial coherence for a tight focusing through the

[8] Author to whom any correspondence should be addressed.

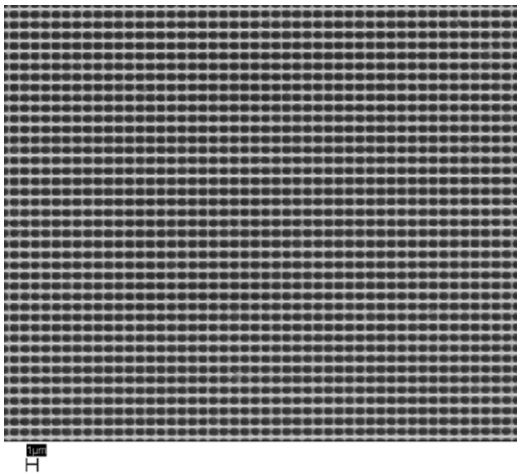

Figure 1. Scanning electron micrograph of the square-lattice 2D silicon photonic crystal slab. The shape of the holes in the silicon top layer is round with a diameter 0.76 μm and with a periodicity of 1 μm. The area of the crystal is 10 mm × 10 mm.

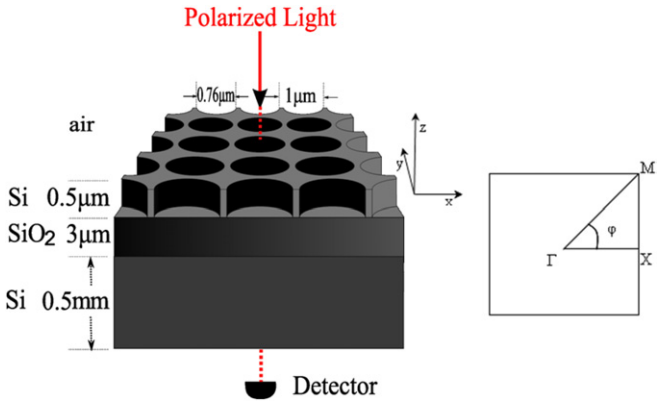

Figure 2. Schematic representation of the photonic crystal slab used to measure the transmission under normal incidence (left). The corresponding irreducible Brillouin zone is spanned by the Γ–X and Γ–M crystal symmetry directions (right).

small crystal area. This is usually not possible with spatially incoherent light, e.g. from incandescent or fluorescent lamp type of sources. As a result, the overall transmission would be low, leading to extended detection times or a low signal-to-noise ratio. We note that this problem becomes even more apparent in the mid-infrared spectral range where the focusability of light is even smaller, where detectors are less efficient, and where noise from thermal background radiation is higher than in the near-infrared and visible spectral range. The small area of the described membranes is typical for the sequential fabrication techniques employed, and when free-standing membranes have to be mechanically stabilized.

Here we characterize the near- to mid-infrared transmission spectra of a large-area (10 mm × 10 mm) silicon PhC slab (see figure 1) fabricated by the laser interference lithography (LIL). This should be of interest for spectral filtering also of low-spatial quality light which is, e.g. important in low-coherence backscattering spectroscopy applications [8]. In the following we present the experimental setup and the experimental transmission data, and we compare the data with the prediction of a theoretical model. To retrieve the centre frequency and quality factor of selected transmission resonances we fit Fano-type resonances on Airy (Fabry–Perot) background to the experimental data.

2. Experimental

The large-area crystal with a high-index contrast based on a silicon-on-insulator (SOI) wafer was available from fabrication with a novel modification of LIL [9], which can also pattern high-index materials. The SOI wafer consists of a 0.5 μm thick top silicon layer, which is separated from the 0.5 mm thick silicon substrate by a low-index buffer layer of 3 μm thick silicon oxide. The silicon wafer and top layer are specified with a resistivity of 8.5–22 $\Omega\,\mathrm{cm}^{-1}$ (see general specifications for 300 nm standard Unibond SOI wafer in [10]). The refractive indices of $n = 3.45$ and 1.45 for Si and SiO_2, respectively, are considered constant over the whole wavelength range investigated here (from 1.1 to 2.4 μm, the refractive index decreases by 3% for Si and by 0.2% for SiO_2). The structure of the investigated 2D-PhC slab is depicted in figure 2, together with the corresponding first Brillouin zone and its Γ–X and Γ–M symmetry directions. The photonic structure fabricated in the top layer is a high-index slab carrying a square pattern of 0.5 μm deep, round air holes with 0.76 μm diameter. A relatively large hole spacing of 1 μm is chosen to provide photonic resonances in the mid-infrared spectral region corresponding to photon energies of less than half of the electronic bandgap of Si [11]. This should also allow later investigations of the third-order ($\chi^{(3)}$-based) non-linear response of the crystal with reduced non-linear loss as can occur through two-photon absorption.

The transmission measurements were performed with a spectrophotometer (Varian, Inc. Cary 5E) in the near- to mid-infrared-wavelength range. The spectral bandwidth of the source was set to 4 nm (at 2 μm wavelength). The far-field beam divergence of the light beam in front of the sample was 4° × 3.4°. In order to allow for a high throughput of light, the rectangular cross section of the light beam was rather large, 2.5 mm × 1.5 mm, however, the beam remained located entirely within the crystal's 10 mm × 10 mm area. A polarizer is placed in front of the crystal to set the polarization. To orient the crystal's hole pattern to a known angle with regard to the polarization direction, the sample is rotated about its surface normal (angle φ in figure 2). The coarse orientation of the x- and y-directions can be seen from the edges of the square-shaped crystal, which is cut approximately parallel to these directions. A few degrees of rotation is then sufficient to orient the diffraction (Laue) pattern obtained with a HeNe laser under normal incidence symmetrically with regard to the direction of the polarizer. Behind the sample the transmitted light is collected by a large-area detector (5 mm × 5 mm). Absolute transmission spectra are obtained by normalizing to the spectrum of the incident light, measured with no crystal in place. With a recording time of a few minutes per spectrum, the spectra show a signal-to-noise ratio of about 100.

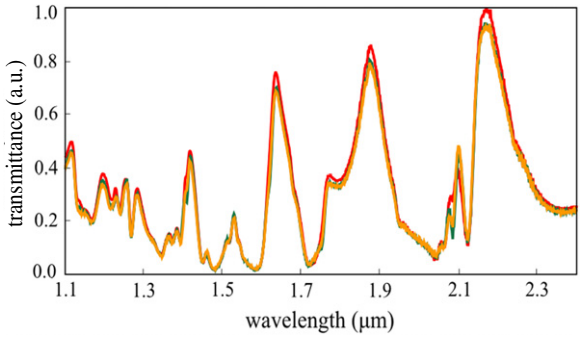

Figure 3. Transmission through the PhC slab measured at normal incidence as a function of wavelength, with the electric field aligned along the Γ–X direction ($\varphi = 0°$, red trace), along an intermediate direction ($\varphi = 22.5°$, green), and along the Γ–M direction ($\varphi = 45°$, orange).

3. Results and discussion

The transmission was measured across the wavelength range from 1.1 to 2.4 μm, thus spanning a range of about 150 THz, at normal incidence to the PhC slab. With such normal incidence, for round holes and 4-fold rotation symmetry, theory predicts a transmission, which is independent of polarization [12]. In order to verify this we have measured three transmission spectra for normal incidence of polarized light, where the alignment of the E-field vector of the light was varied with respect to the crystal symmetry direction. In figure 3, these spectra are displayed, as recorded with the E-field vector aligned at an angle of 45° with respect to the x-axis as given in figure 2 (corresponding to the ΓX direction in reciprocal space, i.e. $\varphi = 0°$, red trace), at an intermediate angle ($\varphi = 22.5°$, green trace), and along the x-axis (Γ–M direction, $\varphi = 45°$, orange trace). As can be seen from figure 3, the spectra are almost identical, with less than 5% deviations in transmission, which confirms the expected polarization independence.

Based on this observation, in the following, we restrict ourselves to the analysis of one of the measured transmission spectra, for which we select the trace with $\varphi = 45°$ (electric field along Γ–M direction) as replotted in figure 4(a). It can be seen that the spectrum consists of a series of broader transmission peaks (e.g. 100 nm bandwidth at around 2.15 μm), which resemble an Airy-type transmission function, on which narrower, Fano-type dispersive features are superimposed (e.g. around 2.1 μm).

The origin of the broader resonances can be attributed to interference in the alternating layers of materials and their respective refractive indices. For instance, the slow variation of transmission along the broad resonances indicates a low quality factor and a wide free spectral range (FSR), which may be addressed to the small thickness of the top and buffer layers and to the well-below-unity Fresnel reflectivity of the involved interfaces.

For a better identification, we calculate the FSR (FSR = speed of light in vacuum/(2 × layer thickness × refractive index)) that corresponds to the effective thickness and index of the three layers. The top layer consists of about 62% Si and 38% air as obtained from the diameter and spacing of

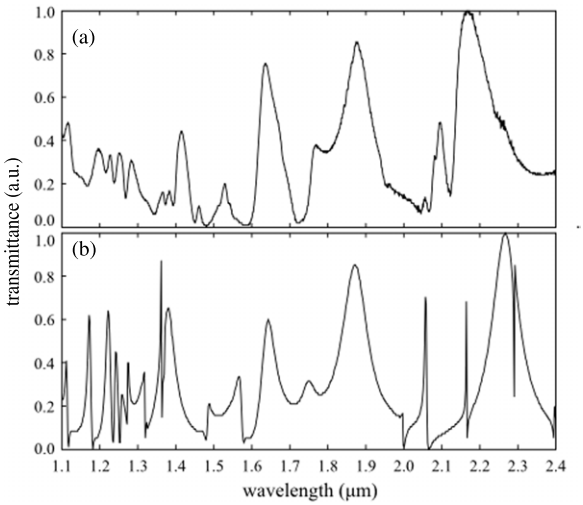

Figure 4. Measured (a) and calculated (b) transmission versus wavelength at normal incidence for linearly polarized light.

the holes in SEM micrographs. Based on effective medium theory [13] this corresponds to an effective refractive index of 2.48. The 0.5 μm thickness of this layer then corresponds to a relatively large FSR of 121 THz and should thus span across the entire recorded range. For the buffer layer where no holes are present [9] we predict a FSR of 33 THz, when using the specifications of the wafer ($d = 3\,\mu$m and $n = 1.45$). The 0.5 mm thick Si thick substrate corresponds to a very small FSR of 0.08 THz.

In comparison, we find in the recorded spectra a spacing between the three main Airy peaks (at 2.15 μm, 1.85 μm and 1.63 μm) of 22.6 THz and 21.9 THz, respectively. These values indicate that the Airy resonances are to be addressed to the buffer layer and suggest a thickness of 4.5 μm for this layer. On the other hand, when looking at the spacing between Airy peaks at higher light frequencies (e.g. at 1.85 versus 1.525 μm, or 1.63 versus 1.42 μm), we find values of 34.6 and 27.2 THz, respectively. This indicates thicknesses of 2.9 μm and 3.7 μm, in better agreement with the wafer specifications (3 μm). The overall variation of the peaks observed across the entire, 150 THz wide recorded spectrum may be addressed to the thin Si top layer, whereas the calculated FSR of the substrate falls well below the resolution of the spectrometer (0.3 THz resolution at 2 μm).

The narrow-band and dispersive features observed in transmission, such as those superimposed on Airy resonances in the range between 2.0 and 2.2 μm wavelength, can be attributed to the photonic structure in the Si top layer [5]. The hole pattern diffracts part of the normally incident (zero in-plane wave vector) light towards the in-plane direction where, at suitable frequencies, leaky modes of the 2D PhC slab can be excited and diffractively radiate back into the normal direction. This corresponds to an additional pathway in transmission at leaky mode frequencies. The superposition of this pathway with the direct transmission then leads to dispersive and asymmetric Fano-shaped resonances.

To model the transmission, we numerically calculated the transmission function using rigorous coupled wave analysis (RCWA) [14]. The transmission was calculated for normal

incidence, with the electric field aligned along the Γ–M direction and with the following parameters as given above, i.e. a hole diameter of 0.76 μm, a periodicity of 1.0 μm, an effective index of 2.48 for the top layer and a 3 μm thick buffer layer. The thickness of the silicon top layer, the index of the buffer layer and the index of the substrate were slightly varied in order to obtain a best fit of the calculated spectrum. A problem is that the very high spectral resolution, as would be required here to well resolve the rather small (0.08 THz) FSR of the thick substrate, would lead to prohibitively long calculation time and memory requirements. On the other hand, for a comparison to our experimental spectra, such high resolution is not required because the experimental resolution (3 THz) averages such fringes out, thereby yielding a constant background from the substrate's Fresnel reflection. Based on these considerations we accounted for the finite experimental resolution with a sufficiently low substrate thickness, and at below 0.01 μm we found only negligible influence on both the Airy-type and Fano-type resonances. Based on these considerations, a constant substrate thickness of 0.01 μm was used for the calculations.

When comparing the calculated transmission spectrum with the experimental one (figure 4), a fair agreement can be seen in the number, position and height of the broader (Airy) features when using for the calculations a top layer thickness of 0.55 μm, a buffer layer index of 1.44 and a substrate index of 3.45. From this we can conclude that the parameters used for the calculation are well suited to describe the overall optical properties of the PhC. One can also find fair agreement in the spectral positions where sharper Fano features are expected: however, the spectral width of the measured resonances is clearly larger than for the perfect (error-free) structure assumed in the calculations. This deviation in linewidth for the Fano resonances thus indicates the strength of errors inherent to our LIL fabrication process.

In order to quantify the influence of these fabrication errors, we determined the quality factor of the measured Fano-shaped resonances (defined as the centre frequency divided by the linewidth) from the experimental spectra by local Fano fits. In previous cases [5, 11, 15, 16] Fano functions were used which assumed a spectrally constant background transmission interfering with the Lorentzian-shaped resonances of leaky modes. Here, however, the observed Fano resonances are clearly located in the wing of broader Airy resonances, i.e. the background transmission cannot be assumed as constant but varies slowly with frequency, thereby modifying the shape of the Fano resonances [17]. In order to account for this with a combined Fano–Airy fit function, we replaced the spectrally constant amplitude of background transmission (see equation (3) in [5]) with the Airy field transmission function [18] for the layer parameters found from the RCWA-fit in figure 4(*b*). The centre frequency, width and amplitude of the Lorentzian component were used as fit parameters. Figure 5 shows an example of such a Fano–Airy fit and it can be seen that there is a good agreement with the experimental line shape. For this resonance, the fit yields a Q-value of 125 and a centre wavelength of 2.12 μm. Similar fits at two further resonances (at 2.05 and 2.08 μm) gave Q-values of 130 and 90, respectively.

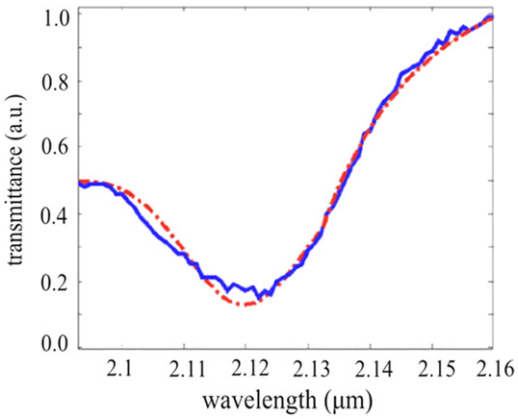

Figure 5. Example of a measured transmission spectrum (solid blue trace) fitted with the superposition of a Lorentz and Airy function (Fano–Airy function, dashed–dotted red trace). The fit yields a Q-value of 125 for the Lorentzian component.

To this end, these Q-values may be compared with what has been previously measured in reflectivity spectra with the same crystal [11]. There, we observed lower Q-values (around 50), which we address to two differences. Firstly, the reflectivity data were obtained only at non-zero angles of incidence, with up to 70°. Also at the smallest angle (10°) the TE and TM spectra had shown a clear difference and, at this angle, the relative spread of the in-plane wave vector is relatively large (30°). This might have reduced the observed Q-value. Here, at normal incidence, there is essentially no polarization dependence (see figure 3). This suggests that no noticeable decrease in the observed Q-values is expected at almost the same beam divergence (here 4° × 3.4°). Secondly, the previously used Fano fits were based on a constant background. Then, a finite slope of background Airy resonances may partly be interpreted as an increased width of the Lorentzian contribution, i.e. as a lowered Q-value.

For a comparison to what Q-values are theoretically expected, we used the finite-difference time-domain (FDTD) method [19]. Here the temporal evolution of a broad-bandwidth light field is calculated and a Fourier analysis yields the frequencies and decay rates of the excited resonances. These calculations reveal the Q-values as given solely by intrinsic losses in an ideal structure, i.e. the maximum achievable values limited only by diffraction at the pattern of holes [20]. For the computations we used again the parameters as in figure 4(*b*); however, with the substrate extending to beyond the computational cell, thereby assuming an infinite thickness. The motivation and justification of this approach follows similar arguments as for a thin substrate in the RCWA calculations.

From the calculations we find intrinsic Q-values, Q_i, ranging from 161 to 358 for the resonances in the wavelength range from 2 to 2.2 μm. The difference in the experimental Q-factors can be addressed to the extrinsic losses, which are associated with the modified LIL fabrication method that is applied here. The component in Q-value which can be assigned to extrinsic losses, Q_e, lies in the order of 200, when considering that intrinsic and extrinsic losses add inversely ($1/Q = 1/Q_\mathrm{i} + 1/Q_\mathrm{e}$) [21].

The reason for extrinsic losses can be caused by irregularities or sidewall roughness [22], tapered sidewalls [23] or out-of-plane scattering [24, 25]. However, recent experiments performed on large structures for the THz range have shown that the most dominant contribution comes from errors in the large-scale periodicity of the hole pattern [26]. These experiments were restricted to a relatively small crystal area of about 20 × 20 periods while the relative fabrication precision of THz PhC slabs is excellent. In contrast, our experiments test a much wider range of large-scale periodicity (up to 10 000 × 10 000 periods) and still yield Q-values that are, within a factor of 1.2–2.5, comparable to the theoretical values. This indicates that the modified LIL fabrication technique used provides an excellent long-range periodicity indeed also over a large area.

4. Summary and conclusions

We have measured the spectral transmission of a large-area (10 mm × 10 mm) two-dimensional silicon photonic crystal slab waveguide in the near- and mid-infrared wavelength range. The crystal slab was fabricated by the LIL using a SOI wafer, and carries a 1 μm period square pattern of round holes in the 0.5 μm thick silicon top layer. Transmission was recorded under normal incidence over the wavelength range from 1.1 μm to 2.4 μm, i.e. from the near-infrared single-photon absorption edge of silicon to below the mid-infrared two-photon absorption edge. We observe Fano and Fabry–Perot-type transmission resonances, which are independent of polarization, i.e. independent of aligning the electric field vector with respect to the crystal symmetry. Position and height of the resonances are in reasonable agreement with predictions based on the RCWA. The width of the measured Fano resonances, which originate from the photonic hole structure and show Q-values between 90 and 130, is typically a factor of 1.2–2.5 above prediction. However, as the Q-values of such resonances seem predominantly susceptible to errors in the long-range periodicity, the present experiments form a test mainly of the long-range periodicity of the modified LIL fabrication used. The associated extrinsic Q-value (in the order of 200) corresponds to an upper limit of 2 nm in the hole period, averaged over the entire crystal. It appears that, indeed, the modified LIL fabrication can maintain periodicity over large ranges (up to 10 mm) and with high fidelity.

The transmission experiment described in this contribution demonstrates the principal suitability of photonic crystal slabs as large-area, high-throughput spectral filters with low periodicity errors. To these advantages add the ease of fabrication from SOI wafers and also their robustness for an uncomplicated handling.

Acknowledgments

The authors acknowledge the support by the Dutch Stichting voor Fundamenteel Onderzoek der Materie (FOM), the Nederlandse Organisatie voor Wetenschappelijk Onderzoek (NWO), the Dutch Ministry of Onderwijs, Cultuur en Wetenschappen (OCW) and the Deutsche Forschungsgemeinschaft (DFG). The authors are grateful to H L Offerhaus, J Herek, A Driessen, M E Klein and C Bostan for stimulating discussions, to M Smithers, M Luttikhof, H van Wolferen, R M de Ridder, C Lee, P van der Slot, P Hartgers (Laser Application Center, LAC), F Ploegman (LAC), H J G van Heel from the Netherlands Centrum voor Laser Research, NCLR employees and the clean room staff of the MESA$^+$ Research Institute for the technical support.

References

[1] Joannopoulos J D, Meade R D and Winn J N 1995 *Photonic Crystals, Molding the Flow of Light* (Princeton, NJ: Princeton University Press)
[2] Suh W, Solgaard O and Fan S 2005 Displacement sensing using evanescent tunneling between guided resonances in photonic crystal slabs *J. Appl. Phys.* **98** 033102
[3] Noda S, Yokoyama M, Imada M, Chutinan A and Mochizuki M 2001 Polarization mode control of two-dimensional photonic crystal laser by unit cell structure design *Science* **293** 1123
[4] Villeneuve P R, Fan S and Joannopoulos J 1996 Microcavities in photonic crystals: Mode symmetry, tunability, and coupling efficiency *Phys. Rev.* B **54** 7837
[5] Fan S and Joannopoulos J D 2002 Analysis of guided resonances in photonic crystal slabs *Phys. Rev.* B **65** 235112
[6] Grillet C, Freeman D, Luther-Davies B, Madden S, McPhedran R, Moss D J, Steel M J and Eggleton B J 2006 Characterization and modeling of Fano resonances in chalcogenide photonic crystal membranes *Opt. Express* **14** 369
[7] Crozier K B, Lousse V, Kilic O, Kim S, Fan S and Solgaard O 2006 Air-bridged photonic crystal slabs at visible and near-infrared wavelengths *Phys. Rev.* B **73** 115126
[8] Kim Y L, Liu Y, Roy H K, Wali R K and Backman V 2005 Low-coherent backscattering spectroscopy for tissue characterization *Appl. Opt.* **44** 366
[9] Prodan L, Euser T G, Wolferen H A G M, Bostan C, Ridder R M, Beigang R, Boller K-J and Kuipers L 2004 Large-area two-dimensional silicon photonic crystals for infrared light fabricated with laser interference lithography *Nanotechnology* **15** 639
[10] SOITEC, Parc Technologique des Fontaines, 38190 Bernin, France: www.soitec.com
[11] Prodan L, Groß P, Beigang R, Kuipers L and Boller K-J 2007 Spectral investigation of a large-area 2D silicon photonic crystal slab for mid-IR radiation *J. Phys. D: Appl. Phys.* **40** 5571
[12] Lousse V, Suh W, Kilic O and Fan S 2004 Angular and polarization properties of a photonic crystal slab mirror *Opt. Express* **12** 1575
[13] Choy T C 1999 *Effective Medium Theory, Principles and Applications* (Oxford: Oxford University Press)
[14] DiffractMOD by RSoft Design Group, Inc: www.rsoftdesign.com
[15] Fano U 1961 Effects of configuration interaction on intensities and phase shifts *Phys. Rev.* **124** 1866
[16] Pacradouni V, Mandeville W J, Cowan A R, Paddon P, Young J F and Johnson S R 2000 Photonic band structure of dielectric membranes periodically textured in two dimensions *Phys. Rev.* B **62** 4204
[17] Mies F H 1968 Configuration interaction theory: effects of overlapping resonances *Phys. Rev.* **175** 164
[18] Hecht E 2001 *Optics Light for a New Age* (Reading, MA; Addison-Wesley)
[19] MIT Electromagnetic Equation Propagation (MEEP): abinitio.mit.edu/wiki/index.php/Meep

[20] Bogaerts W, Bienstman P, Taillert D, Baets R and De Zutter D 2002 Out-of-plane scattering in 1-D photonic crystal slabs *Opt. Quantum Electron.* **34** 195–203

[21] Villeneuve P R, Fan S, Johnson S G and Joannopoulos J D 1998 Three-dimensional photon confinement in photonic crystals of low-dimensional periodicity *IEE Proc.—Optoelectron.* **6** 384

[22] Bogaerts W, Bienstman P and Baets R 2003 Scattering at sidewall roughness in photonic crystal slabs *Opt. Lett.* **28** 689–91

[23] Tanaka Y, Asano T, Akahane Y, Song B S and Noda S 2003 Theoretical investigation of a two-dimensional photonic crystal slab with truncated cone air holes *Appl. Phys. Lett.* **82** 1661–3

[24] Ferrini R, Houdre R, Benisty H, Qiu M and Moosburger J 2003 Radiation losses in planar photonic crystals: two-dimensional representation of hole depth and shape by an imaginary dielectric constant *J. Opt. Soc. Am.* B **20** 469–78

[25] Benisty H, Labilloy D, Weisbuch C, Smith C J M, Krauss T F, Cassagne D, Beraud A and Jouanin C 2000 Radiation losses of waveguide-based two-dimensional photonic crystals: positive role of the substrate *Appl. Phys. Lett.* **76** 532–4

[26] Prasad T, Colvin V L and Mittleman D M 2007 The effect of structural disorder on guided resonances in photonic crystal slabs studied with terahertz time-domain spectroscopy *Opt. Express* **15** 16954–65